

Dual-Mode Filter with High Design Flexibility Using Short-Loaded Resonator

Zhaojun Zhu, Ke Yang, Xiufeng Ren, and Lu Cao

School of Physics

University of Electronic Science and Technology of China, Chengdu, 610054, China
 uestc98@163.com, 18729985221@163.com, 17854227863@163.com, cl_stella@163.com

Abstract — This work presents a series of independent bandpass filters (BPFs) based on dual-mode resonators (DMRs) with short stub-loaded. BPFs conform to the 802.11n protocol and include three passbands with center frequencies and bandwidths of 2.46 GHz, 3.55 GHz and 5.22 GHz, 130 MHz, 130 MHz and 470 MHz. Insertion loss and reflection loss are 1.5 dB, 1.6 dB and 1.3 dB, 18 dB, 20 dB, 30 dB. The filters are useful in the WLAN/WIMAX applications with compact size. According to the current distributions along the resonator, the feed-lines with high design flexibility arms were introduced in order to supply the needed external coupling for the dual-/tri passbands simultaneously, and achieve good impedance matching in each passband. Finally, by the version 15 of High Frequency Structure Simulator (HFSS), three BPFs with single, dual and triple passbands were designed on the Rogers 5880 substrate with the relative dielectric constant $\epsilon_r = 2.2$, substrate loss $\tan\delta = 0.002$, and the thickness $h = 0.508$ mm. The BPFs are measured by Agilent 85058E Vector Network Analyzer (VNA). The measured results have good agreement with the simulated ones.

Index Terms — Bandpass filter, dual-mode resonator, odd and even-mode theory, tri-band filter.

I. INTRODUCTION

Nowadays, the information age is developing rapidly. Bandpass filter (BPF) plays an important role in microwave circuits, which attracts more attentions of the researchers. Wolff first demonstrated a microstrip dual-mode filter in 1972 [1]. Since then, dual-mode microstrip filters have been widely used in communications systems [2–3]. In the past one decade, various of methods to design the multiband filter have been put forward [4–13]. In [6–8], a tri-band BPF comprises two stepped-

impedance resonator (SIRs) with short stub-loaded at the center plane. This method can reduce the overall size of the filter, while always following a larger insertion loss. The tri-band filters [8] which have a wide range of applications for 2.4 GHz, 3.5 GHz, and 5.2 GHz, are designed by using several assembled half-wavelength SIRs without any stub. However, great overall circuit size is inevitable by this way. Furthermore, a tri-band BPF [9] uses a rectangular ring-resonator, its four edges are respectively grounded to form a short stub-loaded, and two opposite sides are added an open stub-loaded. Furthermore, a defected ground structure was adopted to enhance the coupling strength with low insertion loss in [10]. For the above current methods, three major goals need to be achieved, such as compact size, independent control of passband frequencies and low insertion loss.

This letter proposes three folded dual-mode resonator structures based on SIR (DMR 1, DMR 2, and DMR 3). The center frequencies of SIR are prospectively based on even-odd-mode analysis. In addition, several high design flexibility arms structures are introduced to enhance the coupling between resonators and feed-lines. Finally, three BPFs with single, dual, and triple passbands were individually designed, fabricated, and measured.

II. DESIGN OF THE DUAL-MODE RESONATOR

The schematic diagram of the dual-mode resonator (DMR) 1 is shown in Fig. 2 (a), which consists of a half-wavelength resonator and a short-loaded. This DMR is denoted by lengths ($L1$, $L2$) and widths ($W1$) with a short-circuited stub perturbation with length ($W2$) and width ($W3$) at the center plane. The even-odd-mode method can be applied to the equivalent circuits because of the symmetrical structure.

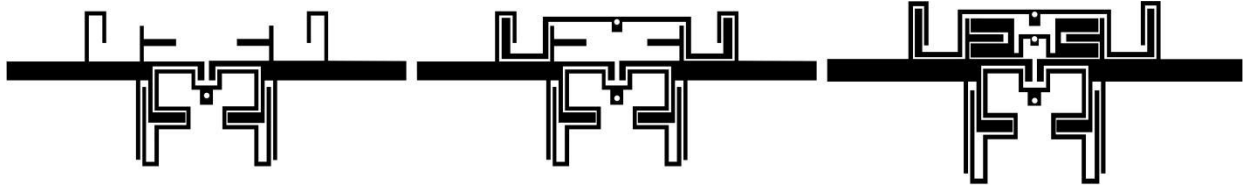


Fig. 1. (a) Schematic diagram of the proposed BPF 1, (b) schematic diagram of the proposed BPF 2, and (c) schematic diagram of the proposed BPF 3.

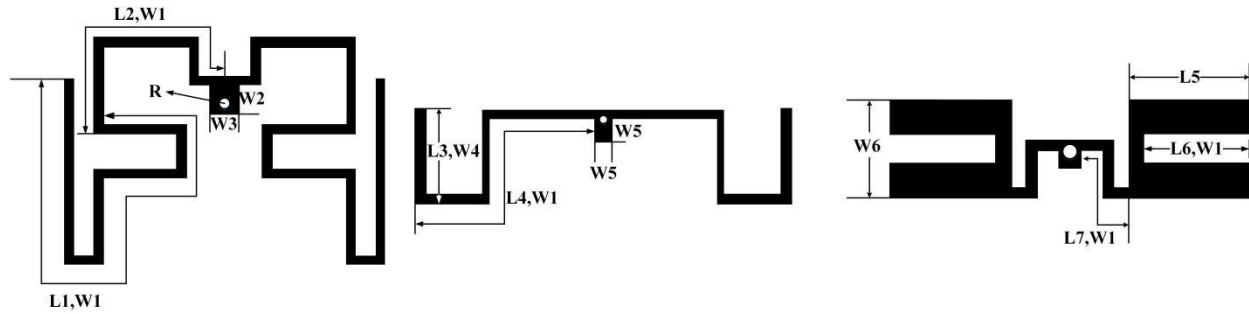


Fig. 2. (a) Schematic diagram of the proposed DMR 1, (b) schematic diagram of the proposed DMR 2, and (c) schematic diagram of the proposed DMR 3.

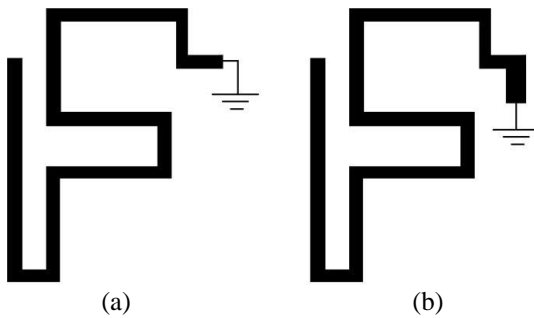


Fig. 3. DMR analysis using the even-odd-mode method: (a) equivalent circuit in the odd-mode, and (b) equivalent circuit in even-mode.

The commercially available full-wave electromagnetic simulators HFSS were used to characterize the electric field patterns for the dual-mode resonator. HFSS uses the finite element method (FEM) to analyze the electromagnetic characteristics of 3D objects. The basic process of solving the problem by FEM includes three parts, which are the mesh discretization of the object, the solution of the simultaneous matrix equations related the mesh and the postprocessing calculation of the problem.

It can be seen that the whole structure is symmetrical with the center point, so the center point is modeled as the origin point and the mirror operation is applied. The physical excitation of the filter is by the coaxial line with the TEM wave. In order to use the wave-guide port in the simulation code, the port surface must cover more than

ninety-five percent of the TEM field. It is assumed that the width of the excitation microstrip is w and the thickness of the dielectric layer is h . The height of the wave port is generally set to $6-10h$. When $w > h$, the width of the wave port is set to about $10w$; when $w < h$, the width of the wave port is set to about $5w$. Finally, the height and width of the wave port of are $10h$ and $10w$ in this paper.

According to the standard which is set up by user, HFSS simulation code uses adaptive mesh generation technology. The solution frequency of the meshing is generally set at the center frequency of the filter. After each new mesh subdivision, HFSS will compare the results of the S parameters with the old one. If the error is less than the set criterion, it is shown that the result is convergent and the adaptive process will end. The dimensions are optimized by a full-wave simulation to take all the discontinuities into consideration.

The symmetrical plane can be modeled, as an electric wall (E. W.) with the equivalent circuits in Fig. 3 (a) under odd-mode excitation, while as an magnetic wall (M.W.) under the odd-mode excitation in Fig. 3 (b). Therefore, the odd-mode resonant frequency f_{odd} and even-mode resonant frequency f_{even} can be determined by the L_{odd} and L_{even} , respectively, which can be expressed approximately as:

$$L_{odd} = 2L_1 + 2L_2, \quad (1)$$

$$L_{even} = 2L_1 + 2L_2 + W_2. \quad (2)$$

Then the odd-mode frequency f_{odd} and the even-mode frequency f_{even} can be expressed as:

$$f_{odd} = \frac{c}{L_{odd} \sqrt{\epsilon_{eff}}}, \quad (3)$$

$$f_{even} = \frac{c}{L_{even} \sqrt{\epsilon_{eff}}}, \quad (4)$$

where c is the speed of light, and ϵ_{eff} is the effective dielectric constant of the substrate.

III. DESIGN OF THE PROPOSED FILTERS

The coupling scheme of the single-band filter based on DMR1 and complex feed-lines is shown in Fig. 4.

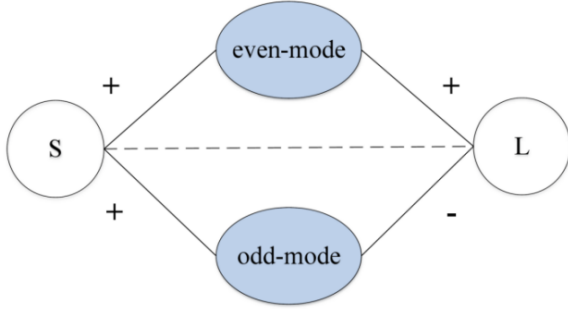


Fig. 4. Coupling structure of the proposed single-band BPF I.

The signal is coupled to two modes at the same time, providing two main paths between the source and load, and there is no coupling between each mode. Two transmission zeros can be created near passband due to the two mainly signals path and source-load coupling (S-L coupling) counteraction. The coupling matrix can be written down as:

$$\begin{bmatrix} 0 & M_{Se} & M_{So} & M_{SL} \\ M_{eS} & M_{ee} & 0 & M_{eL} \\ M_{oS} & 0 & M_{oo} & M_{oL} \\ M_{LS} & M_{Le} & M_{Lo} & 0 \end{bmatrix}.$$

In this coupling matrix, the subscript of e and o refer to the even- mode and odd- mode, separately, while the subscript of S and L refer to the source and the load. Since the proposed single-band filter exhibits symmetry property, the relationship $M_{eS} = M_{eL}$, and $M_{oS} = -M_{oL}$ establishes. The gap between source and load S_o is introduced to provide proper S - L coupling coefficient M_{SL} for generating an additional zero. In order to get coupling matrix, an example is taken of a second order generalized Chebyshev filter with the center frequency of 2.4 GHz, the 3 dB bandwidth of 130 MHz, the return loss of 28 dB and two trans-mission zeros frequencies locate at 1.7 and 2.9 GHz. The corresponding coupling coefficients [14] are:

$$\begin{bmatrix} 0 & 0.79976 & 0.88523 & 0.025 \\ 0.79976 & -1.5551 & 0 & 0.79976 \\ 0.88523 & 0 & 1.5551 & -0.88523 \\ 0.025 & 0.79976 & -0.88523 & 0 \end{bmatrix}.$$

IV. RESULT AND DISCUSSION

In Fig. 2 (a), the length W_2 does not affect the odd-mode resonant frequency, whereas the even-mode is directly depend on the length W_2 , to observe the mode splitting, the dual-mode resonators have been simulated with vary loaded size. As shown in Fig. 5 (a), when W_2 increases from 0.4 to 1.2 mm (the others are as $L_1 = 15.75$ mm, $L_2 = 8$ mm, $W_1 = 0.3$ mm, $W_3 = 1$ mm, $R = 0.2$ mm), the resonant frequency of the even mode decreases from 2.35 GHz to 2.29 GHz, while that of the odd mode hardly changes. The line lengths L_1 and L_2 affect both the even- and odd-mode resonant frequencies. Figure 5 (b) depicts that the even- and odd-mode resonant frequencies vary with L_1 . When L_1 increases from 13.75 mm to 15.75 mm (the others are as $L_2 = 8$ mm, $W_1 = 0.3$ mm, $W_2 = 0.9$ mm, $W_3 = 1$ mm, $R = 0.2$ mm), the resonant frequency of the even mode decreases from 2.42 GHz to 2.26 GHz, while that of the odd mode decreases from 2.52 GHz to 2.35 GHz, and it is obvious that two curves are almost parallel lines. From the above two diagrams, it can be seen that desired center frequency can be regulated by changing the length of SIR and the shorted stub.

The structure of the proposed single-band filter I is shown in Fig. 1 (a). It consists of a DMR with the S - L coupling. Since the DMR 1 locates at the down side of the feed lines, another DMR is added to work on 3.5 GHz to get a dual-band filter and make full use of the space of the structure. Moreover, because of the special of the structure, the two DMRs can be individually designed. Fig. 6 gives the curves about 3 situations: with DMR 1, with DMR 2 and with two DMRs. Figure 1 (b) depicts the layout of the proposed dual-band BPF II. DMR 1 and DMR 2 are distributed over the upper and lower sides of the feed lines, and we can see that DMR 2 is a structure similar to DMR 1. Similarly, DMR 3 (seen in Fig. 1 (c)) can be added into the dual-band BPF, and the tri-band BPF can be gained finally. Thus, the current distributions of the proposed tri-band BPF at the center frequency of each passband are demonstrated in Fig. 7. There is a strong current path for the DMR at its center frequency, while the other DMRs exhibit a weak current distribution. The main reason for the current path is that there is almost no coupling between these DMRs. The three DMRs are independent of each other and do not interfere with each other, so a strong current appears in one DMR at its center frequency point, while that in other DMRs is weak.

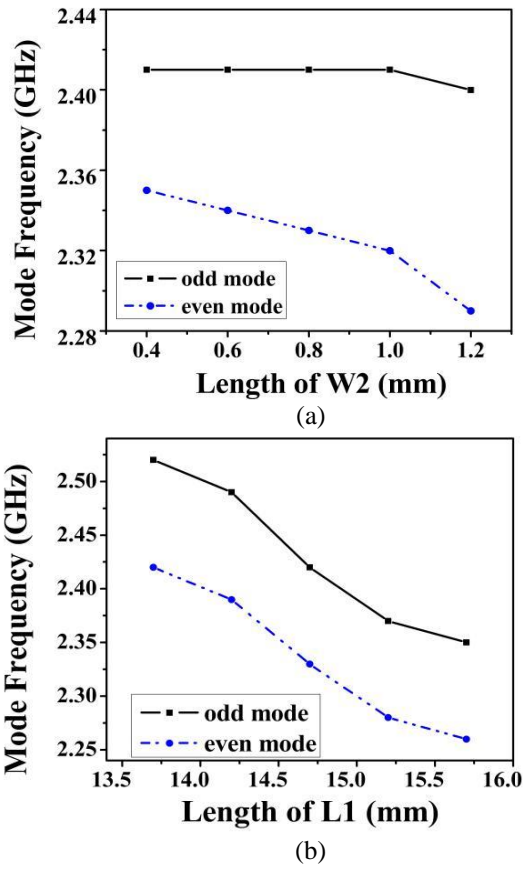


Fig. 5. Variation of even-odd-mode resonant frequency on W_2 (a) and L_1 (b).

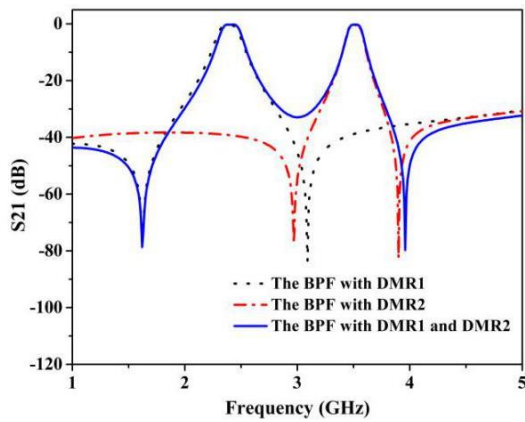


Fig. 6. The simulation of S₂₁ parameter of the dual-band BPF II with DMR 1, DMR 2, DMR 1 and DMR 2.

The geometrical dimensions of proposed filter III are decided as $L_1 = 15.75$ mm, $L_2 = 8$ mm, $L_3 = 3.3$ mm, $L_4 = 11.8$ mm, $L_5 = 3.3$ mm, $L_6 = 2.9$ mm, $L_7 = 2.6$ mm, $W_1 = 0.3$ mm, $W_2 = 0.9$ mm, $W_3 = 1$ mm, $W_4 = 0.5$ mm, $W_5 = 0.8$ mm, $W_6 = 2.7$ mm, $R = 0.2$ mm, and the compact sizes are about $0.2 \times 0.13 \lambda_g$.

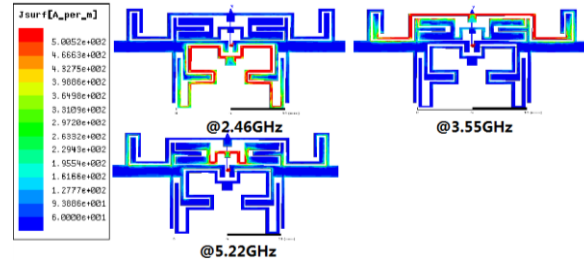


Fig. 7. Current distribution of the proposed tri-band BPF III.

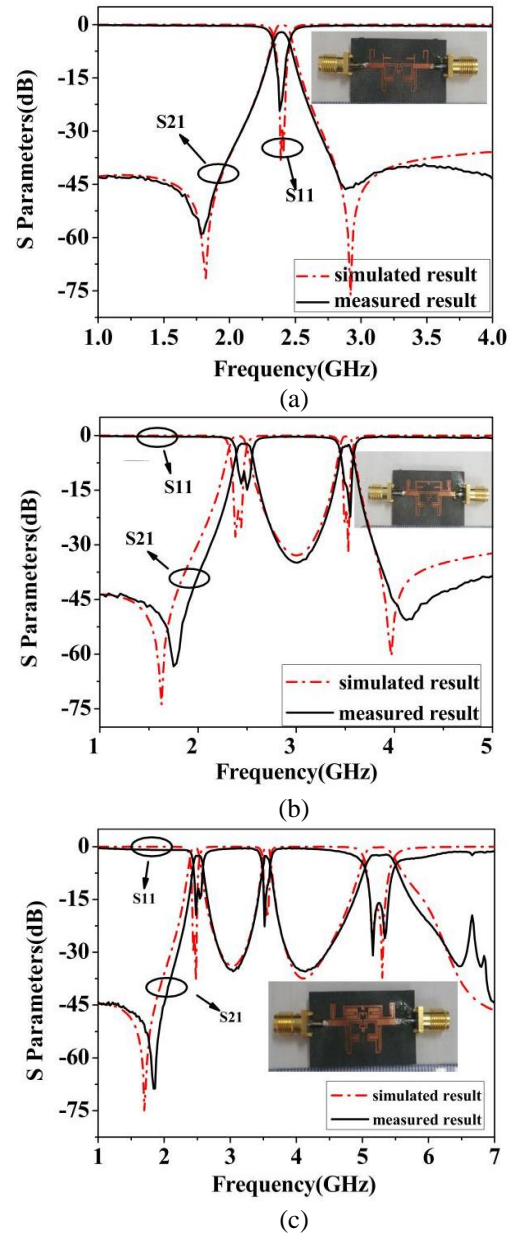


Fig. 8. Simulated and measured results: (a) of the proposed single-band BPF I, (b) of the proposed dual-band BPF II, and (c) of the proposed tri-band BPF III.

Figure 8 depict the results of simulated and measured, the red curves represent the simulated results, while the black curves stand for the measured results. It can be seen the measured results meet the simulated ones very well. Tables 1, 2 and 3 show detailed design specification of BPF I, II, and III. f_0 infers to center frequency of every passband. BW indicates the bandwidth, IL and RL stand for insertion and reflection loss, separately. For the comparison with the previous investigations, Table 4 summarizes some dual-mode BPF performance characteristics. From the Table 4, it can be seen that the presented tri- band BPF shows miniature size with good performances when compared with the previous works.

Table 1: Design specifications of the filter I

Results	f_0 /GHz	BW/MHz	IL/dB	RL/dB
Sim.	2.4	130	0.21	35
Mea.	2.4	120	1	21

Table 2: Design specifications of the filter II

Results	Bands	f_0 /GHz	BW/MHz	IL/dB	RL/dB
Sim.	Band I	2.4	180	0.2	29
	Band II	3.51	130	0.26	31
Mea.	Band I	2.45	180	1.1	14
	Band II	3.51	130	1.5	20

Table 3: Design specifications of the filter III

Results	Bands	f_0 /GHz	BW/MHz	IL/dB	RL/dB
Sim.	Band I	2.4	150	0.3	35
	Band II	3.5	130	0.4	18
	Band III	5.2	470	0.21	35
Mea.	Band I	2.46	130	1.5	18
	Band II	3.55	130	1.6	20
	Band III	5.22	470	1.3	30

Table 4: Comparison between the reference filters and the proposed filter III

References	f_0 /GHz	IL/dB	RL/dB	Filter Size ($\lambda_g \times \lambda_g$)	FBW/%
6	1.57/2.45/5.25	1.5/1.34/0.908	16/16/17	0.182×0.26	8.2/7.3/9.9
7	1.8/2.4/5.8	1.5/0.9/2.9	15/23/18	0.16×0.17	8.9/12.5/5.3
9	1.5/2.45/3.5	1.17/1.02/2.17	19/20/19	0.28×0.11	7.5/5.8/3.6
10	1.8/3.5/5.8	0.88/1.33/1.77	21/15/15	0.108×0.521	7/5/3.5
11	1.52/3.42/5.31	2.6/2.3/5.3	15/35/10	0.36×0.38	5.9/5.8/4
This work	2.46/3.55/5.22	1.5/1.6/1.3	18/20/30	0.2×0.13	5.3/3.7/9

V. CONCLUSION

In this paper, a kind of folded short-loaded dual-mode resonators are proposed. By controlling length ratios of stepped-impedance resonator and shorted stub, three passbands with two poles can be controlled independently in an appropriate range. Finally, three filters, conforming 802.11n protocol, are designed and fabricated on the Rogers 5880 substrate with the relative dielectric constant $\epsilon_r = 2.2$, substrate loss $\tan\delta = 0.002$, and the thickness $h = 0.508$ mm. It is shown that the proposed BPFs have the advantages of good performance. The insertion losses of measured are lower than 2 dB, the frequencies can be tuned conveniently and independently. Good agreement can be achieved between measured results and simulated ones. Based on the above analysis, it can be concluded that our design is attractive for multiband wireless communication.

ACKNOWLEDGMENT

This work is supported by Sichuan Science and Technology Program (Grant No.2020YJ0271).

REFERENCES

- [1] I. Wolff, "Microstrip bandpass filter using degenerate modes of a microstrip ring resonator," *Electron. Letters*, vol. 8, no. 12, pp. 302-303, June 1972.
- [2] B. F. Ganji, M. Samadbeik, A. Ramezani, and A. Mousavi, "Simple configuration low-pass filter with very wide stop band," *Applied Computational Electromagnetics Society Express Journal*, vol. 1, no. 1, pp. 4-7, 2016.
- [3] X. Deng, K. D. Xu, Z. Wang, and B. Yan, "Novel microstrip ultra-wideband bandpass filter using radial-stub-loaded structure," *Applied Computational Electromagnetics Society Express Journal*, vol. 1, no. 1, pp. 20-23, 2016.
- [4] R. Yin, W. Feng, and W. Che, "High selectivity dual-band bandpass filters using dual-mode resonators," *Applied Computational Electromagnetics Society Journal*, vol. 32, no. 9, pp. 800-805, 2017.
- [5] F. Xia, Q. Zhang, and Y. Chen, "Dualband filter using stub-loaded resonators," *2018 International Applied Computational Electromagnetics Society*

- Symposium-China (ACES-China)*, pp. 1-2, 2018.
- [6] C.-H. Lee, C.-I. G. Hsu, and H.-K. Jhuang, "Design of a new tri-band microstrip BPF using combined quarter-wavelength SIRs," *IEEE Microwave & Wireless Components Letters*, vol. 16, no. 11, pp. 594-596, 2006.
- [7] Q. Li, Y. H. Zhang, X. Feng, and Y. Fan, "Tri-band filter with multiple transmission zeros and controllable bandwidths," *International Journal of Microwave & Wireless Technologies*, vol. 8, no. 1, pp. 9-13, 2016.
- [8] F. C. Chen and Q. X. Chu, "Design of compact tri-band bandpass filters using assembled resonators," *IEEE Transactions on Microwave Theory & Techniques*, vol. 57, no. 1, pp. 165-171, 2009.
- [9] S. J. Sun, T. Su, K. Deng, B. Wu, and C. H. Liang, "Shorted-ended stepped-impedance dual-resonance resonator and its application to bandpass filters," *IEEE Transactions on Microwave Theory & Techniques*, vol. 61, no. 9, pp. 3209-3215, 2013.
- [10] S. Zhang and L. Zhu, "Compact tri-band bandpass filter based on $\lambda/4$ resonators with U-folded coupled-line," *IEEE Microwave & Wireless Components Letters*, vol. 23, no. 5, pp. 258-260, 2013.
- [11] B. Peng, S. Li, B. Zhang, and S. Wang, "Triband filter with high design flexibility and wide stopband using DGS and shorted stub-loaded resonator," *Microwave and Optical Technology Letters*, vol. 57, no. 5, pp. 1226-1228, 2015.
- [12] Z. Zhu, S. Liang, and C. Wei, "Novel pentagonal dual-mode filters with adjustable transmission zeros," *Applied Computational Electromagnetics Society Journal*, vol. 31, no. 10, pp. 1238-1243, 2016.
- [13] X. B. Wei, Y. Shi, P. Wang, J. X. Liao, Z. Q. Xu, and B. C. Yang, "Compact dual-band bandpass filter with improved stopband characteristics," *Electronics Letters*, vol. 48, no. 12, pp. 704-705, 2012.
- [14] J. S. G. Hong and M. J. Lancaster, *Microstrip Filters for RF/Microwave Applications*. 2nd Edition, John Wiley & Sons, 2001.



Zhaojun Zhu was born in Sichuan, China, in 1978. He received the B.S. degree and the Ph.D. degree in Physical Electronics in University of Electronic Science and Technology of China (UESTC), Chengdu, in 2002 and 2007 respectively. Since 2012, he has been an Associate Professor with the UESTC. His research interests include the design of microwave and millimeter-wave circuits.



Ke Yang was born in Shannxi, China, in 1996. He received the B.E. degree in Communication Engineering in Xian University of Science and Technology in 2019, and is working toward the M.A. Eng. degree in UESTC. His research interests include millimeter-wave circuit and phased array wave control algorithm design.



Xiufeng Ren was born in Shandong, China, in 1995. She received the B.E. degree in Communication Engineering in China University of Petroleum in 2018, and is working toward the M.A. Eng. degree in UESTC. Her research interests include antenna design and phased array wave control algorithm design.



Lu Cao was born in Jiangxi Province, China, in 1993. She received the B.S. degree in Physics from Gannan Normal University, in 2015, and M.D. degree in UESTC in 2018. Her research interests include the design of microwave and millimeter-wave circuits.